BIOCHIP JOURNAL, Vol. 3, No. 2, 119-124, June 2009

Fluorescence Imaging of the Spatial Distribution of Ferric Ions over Biofilms Formed by *Streptococcus mutans* under Microfluidic Conditions

Wahhida Shumi[1], Jeesun Lim[2], Seong-Won Nam[2], So Hyun Kim[2], Kyung-Suk Cho[1], Juyoung Yoon[2] & Sungsu Park[2]

[1]Department of Environmental Science and Engineering, Ewha Womans University, Seoul 120-750, Korea
[2]Department of Chemistry and Nano Science (BK21), Ewha Womans University, Seoul 120-750, Korea
Correspondence and requests for materials should be addressed to S. Park (nanopark@ewha.ac.kr)

Accepted 13 April 2009

Abstract

***Streptococcus mutans*, which is an initial dental plaque colonizer on the mucosal surface of oral cavities, utilize exogenous sucrose as a nutrient source to produce extracellular polysaccharides (EPS). EPS are highly sticky and allow bacterial cells to attach to the tooth surface. Bacteria, including *S. mutans*, acquire iron from the human body to survive. However, little is known about the mechanism of iron acquisition during the formation of *S. mutans* biofilms. In this study, we utilized a microfluidic device that generated the microfluidic condition often found in teeth and imaged the spatial distribution of ferric ions over *S. mutans* biofilms formed in the device using a ferric chemosensor. Our results showed that under iron-repleted conditions *S. mutans* produced a lower amount of EPS and thus formed smaller biofilms compared to under iron-depleted conditions, indicating that biofilm formation is not required for the survival of the microorganism in the presence of a sufficient amount of iron. Spatial imaging of the biofilms using a ferric chemosensor revealed that higher amounts of ferric ions accumulated in the inner EPS layer of the biofilm formed under both iron-depleted and iron-repleted conditions, suggesting that the EPS layer in the biofilm is responsible for acquiring and delivering ferric ions to the cell body.**

Keywords: *Streptococcus mutans*, Chemosensor, Ferric ion, Biofilm, Imaging

Introduction

Dental caries is one of the most prevalent diseases in humans and results from acid production in bacterial biofilms that form on the tooth surface[1,2]. Residential microflora on the teeth form biofilms, which cause localized destruction of the teeth[3,4]. The major component of the biofilm matrix is composed of a wide variety of organic materials including exopolysaccharides (ESP), proteins, nucleic acids, etc[5-8]. EPS plays important roles in biofilm formation by enhancing cell adhesion, aggregation, and biofilm structure, etc[9,10].

Among the microflora, *Streptococcus mutans* is the initial dental plaque colonizer on the mucosal surface of oral cavities[8] and it utilizes exogenous sucrose[11] as a nutrient source to produce EPS, which allow bacteria to attach to the tooth surface[2]. Both EPS production and biofilm formation are greatly inhibited in iron-repleted conditions, suggesting that both EPS and the presence of the biofilm are important components in acquiring iron for the microorganism when the availability of iron in the environment is scarce including the mouth. Iron is an essential microelement for all forms of life. Its solubility and bioavailability varies depending on various conditions, and are extremely low under aerobic conditions at physiological pH[12,13]. Bacteria, including *S. mutans*, acquire iron from the human body to survive. Extracellular iron (Fe^{3+}) is transported into bacterial cells by binding to negatively charged functional groups on the EPS layer[14]. Thus, EPS production is greatly enhanced when the availability of ferric ions (Fe^{3+})[15] are limited. Although the iron acquisition mechanism has been determined in many microorganisms by measuring the total amount of iron accumulated in the biofilm, the exact spatial distribution in the bulky biofilm architecture has not been reported *in situ*. Previous studies have demonstrated that fluorescently labeled ferrichrome analogs were useful tools in the study of microbial iron utilization and detection in living cells[16,17]. However, this tool has not yet been exploited to study the distribution of iron in biofilms.

Previously, we described a novel fluorescent chemosensor that was quenched upon binding to ferric

Table 1. pH and optical density of *S. mutans* with different growth types under iron-depleted (TSB) and iron-repleted (TSB+100 μM ferric sulfate) conditions at the different periods of incubation.

Growth type		TSB medium (control)			TSB medium with ferric sulfate		
		Day 1	Day 2	Day 3	Day 1	Day 2	Day 3
Planktonic	pH	5.8	5.0	4.6	5.4	5.0	4.6
	OD	1.1±0.9	1.9±0.8	1.9±1.3	0.9±0.8	1.8±1.4	1.9±1.2
Sessile	pH	6.2	5.6	4.6	5.7	5.2	4.6

ion and regained its fluorescence upon dissociation of the metal ion[18]. Most recently, we also demonstrated that a microfluidic device can be used to quantify EPS production in biofilms formed under laminar flow[19]. In this study, we report *in-situ* imaging of the spatial distribution of ferric ion accumulated in the biofilm formed by *S. mutans* under lamina flow using the chemosensor and microfluidic device. By analyzing the distribution of ferric ions in a biofilm, we were able to show that the outer EPS layer in the biofilm has a higher concentration of ferric ion and plays an important role in adsorbing free ferric ions from its surrounding.

Results and Discussion

pH Changes during the Culture

Since the fluorescence intensities of many fluorescent dyes are affected by changes in pH, it was necessary to confirm that there would be no significant difference in pH between bacterial cultures with and without ferric ions. Although the bacterial cultures became acidic over time, there was no significant difference in pH between the two culture conditions (Table 1). The fluorescence intensity of the chemosensor was determined to be 58.9 and 55.2 at pH 5.0 and pH 4.5, respectively, whereas, in presence of 100 μM ferric sulfate the fluorescence intensity decreased to 28.8 and 24.3 at the same pH level. This result suggests that the presence of ferric sulfate significantly decreased the fluorescence intensity, as shown in Figure 1C and D.

Initial Biofilm Formation of *S. mutans* was Inhibited under the Iron-Depleted Conditions

CLSM images (Figure 2) show EPS and live cells stained with Con A-Rho and SYTO16, respectively, in absence or presence of ferric sulfate on day 3 of incubation. SYTO16 staining shows that biofilms (Figure 2C), in the absence of ferric sulfate, were larger than those (Figure 2F) formed in the presence of metal ions. Similarly, the images (Figure 2B and E) obtained from the biofilms stained with Con A-Rho

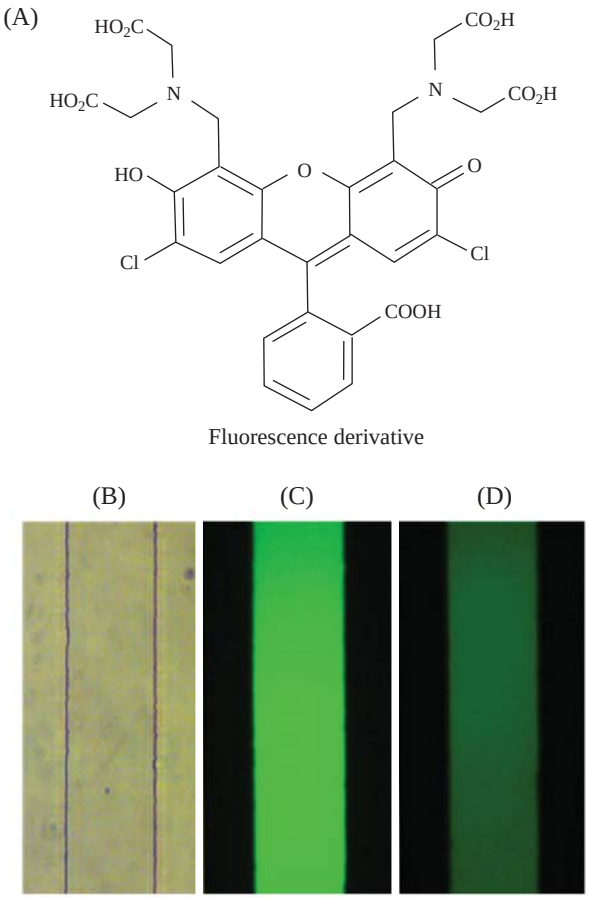

Figure 1. Chemical structure (A) and flurescence intensity of the ferric chemosensor with and without ferric ions in the microchannel (B-D). Optical images of the microchannel filled with the ferric chemosensor (B). C shows a fluorescence image of the microchannel filled containing only 1 μM ferric chemosensor, while D shows a fluorescence image of the microchannel filled with both 1 μM ferric chemosensor and 100 μM ferric sulfate at pH 5.

indicate that a higher amount of EPS was produced in the absence of ferric sulfate than in the presence of metal ions. Optical images (Figure 2A and B) indicate that the biofilm surface area in the absence of ferric sulfate was larger than that in the presence of metal ions. Similarly, EPS production and live cells

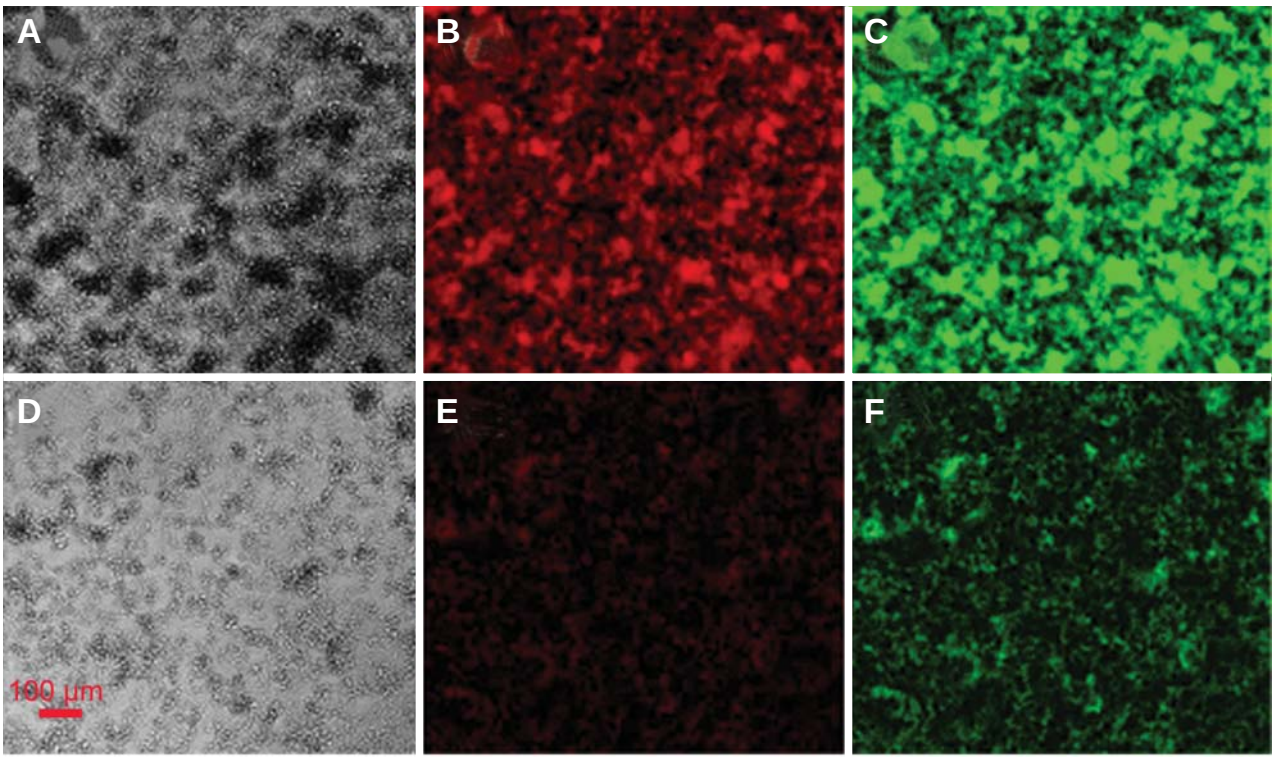

Figure 2. CLSM images show EPS and live cells in *S. mutans* biofilms formed under iron-depleted and iron-repleted conditions at 3 days of incubation. The biofilms in the top row (A-C) were formed under the iron-depleted condition (TSB only), while the biofilms in the bottom row (D-F) were formed under the iron-repleted condition (TSB+100 µm $Fe_2(SO_4)_3$). A and D images are optical images showing the overall structure of the biofilms formed in both conditions. B and E images were obtained from the biofilms stained with Con A-Rho, which indicates EPS production in the biofilms. C and F images were obtained from the biofilms stained with SYO16, which represents live cells in the biofilms. The scale bar is 100 µm.

in the biofilm formed during various incubation periods were visualized with dye staining and CLSM imaging. The light intensity in the images was quantified and analyzed using the Image J program. As shown in Table 2, the red fluorescence signal (9.8) obtained from the biofilms in the absence of ferric sulfate at day 1 was three times higher than that (2.9) of EPS obtained from the biofilms under the same conditions except in the presence of ferric ion. The difference in EPS production between the two culture conditions became smaller as the incubation periods were extended to 2 and 3 days; however, ferric ions were still effective in inhibiting EPS production.

Similarly, the biofilms formed in the presence of ferric ions contained a smaller number of live cells compared to those in the absence of metal ions. This difference was most prominent at day 1. Based on these results, we hypothesize that a smaller number of cells were converted into the sessile stage from the planktonic stage in the presence of ferric ions.

Table 2. Quantitative data of fluorescence intensity obtained from the fluorescence images in Figure 2 shows the relative amounts of live cells and EPS in the biofilms formed during the different periods of incubation under iron-depleted and iron-repleted conditions, respectively. All averages and standard deviations were obtained form three independent experiments.

Culture condition	Incubation periods	Live cells	EPS production
Iron-depleted	Day 1	22.8±1.7	9.8±1.9
	Day 2	24.2±1.8	22.6±1.4
	Day 3	29.5±0.9	24.2±1.8
Iron-repleted	Day 1	5.8±1.5	2.9±0.5
	Day 2	7.1±2.6	9.9±0.3
	Day 3	16.4±0.2	14.2±0.5

Spatial Distribution of Ferric Ions in the Biofilms

CLSM images (Figure 3) of biofilms stained with the ferric chemosensor show that ferric ions accumulated on the inner EPS layer in the biofilm irrespec-

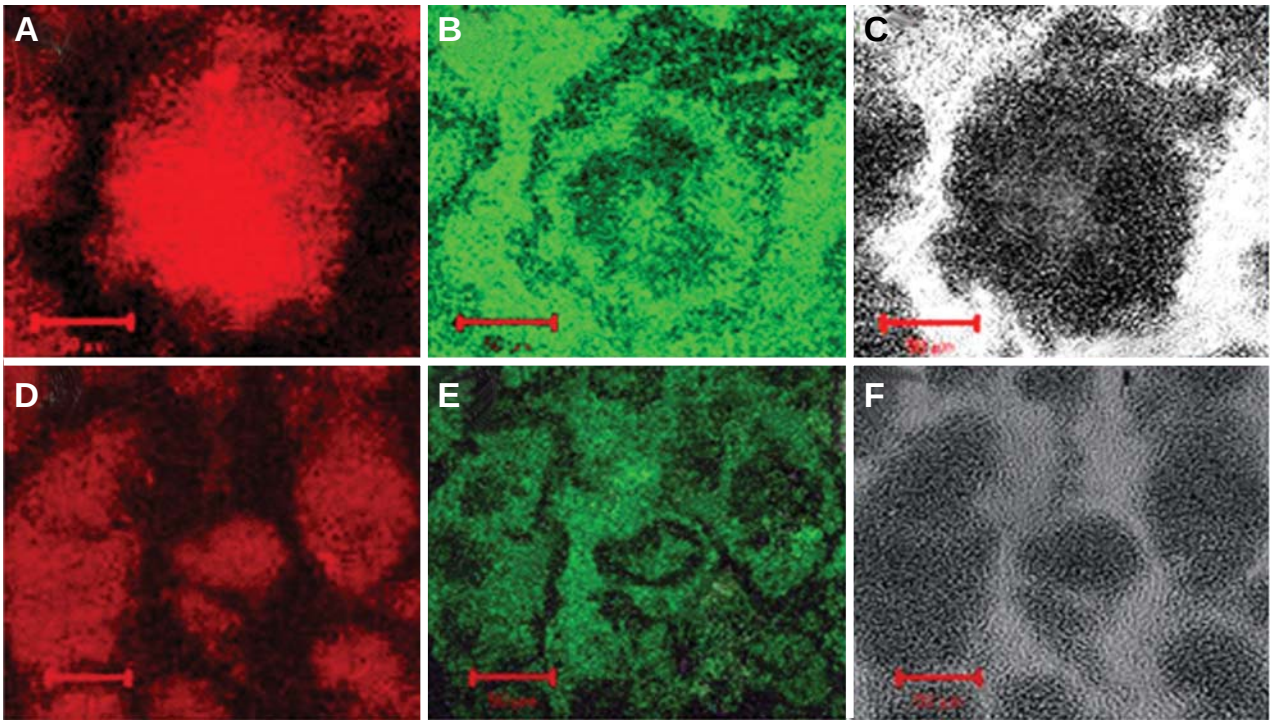

Figure 3. CLSM imaging of the ferric ion and EPS distributions in *S. mutans* biofilm formed under iron-depleted (A-C) and iron-repleted (D-F) conditions at 3 days of incubation. Red fluorescence was obtained from the biofilms stained with Con-A Rho, which is known to specifically bind to EPS. Green fluorescence was obtained from the same biofilms stained with the ferric chemosensor. The optical images of both biofilms are shown in image C and F. The scale bars are 50 μm.

tive of the presence of ferric sulfate. As expected, the biofilms (Figure 3D) at day 3 in the presence of ferric sulfate produced less amount of EPS compared to those (Figure 3A) formed in the absence of metal ions. This EPS production pattern at the two different iron conditions was further supported by the optical images (Figure 3C and F). As expected, ferric ions accumulated in the inner EPS layer of the biofilms under the iron-repleted conditions, which were indicated by clear dark rings. The dark ring seemed to be formed by quenching of the ferric chemosensor due to binding with absorbed ferric ions. Surprisingly, the biofilms under the iron-depleted condition were able to absorb ferric ions from the medium, which was shown by the pale dark rings in the inner EPS layer. Taken together, these data suggest that the EPS layer plays an important role in transporting ferric ions to the cells in the biofilm and the amount of EPS production was inversely dependent upon the amount of available ferric ions.

Conclusions

Fe is the essential micronutrient for most bacterial pathogens. In the extracellular environment, the concentration of free iron is 10^{-18} μM[13], which is far lower than that (10^{-7} μM) required for the growth of bacteria. Upon entering a mammalian host, bacteria suffer from iron-depleted *in vivo* conditions and have managed to adapt to this condition for their survival. These bacteria survive under these conditions by synthesizing iron-specific receptors and different iron-transport systems. Since *S. mutans* require 0.1 to 1.0 μM iron for their growth and to form aggregates, they have to develop iron acquisition systems once they are subjected to *in vivo* conditions. Biofilm formation may be a vital part of the acquisition system. In this study, we showed that *S. mutans* formed biofilms to effectively absorb ferric ions from their surroundings. With the use of the ferric chemosensor, we found that the bioaccumulation of ferric ions in the biofilm was most evident in the inner EPS layer. These results suggest that *S. mutans* biofilms act as biofilters for collecting free ferric ions from the flow.

Materials and Methods

Bacterial Strains and Chemicals

The bacterial strain *Streptococcus mutans* ATCC

3065 was used in this study. The bacterial culture was prepared by inoculating the strain into 10 mL tryptic soy broth (TSB) (Sigma) that was supplemented with 100 μM sucrose and incubating at 37°C overnight. Brain-heart infusion agar (Difco) was used for maintaining the culture by subculture every week. $Fe_2(SO_4)_3$ (final. conc. 100 μM) was added to the TSB only when the effects of ferric ion on the biofilm was examined. Tetramethylrodamine conjugated with conconavalin A (Con A-Rho) (final. conc. 20 μg mL^{-1}) (Invitrogen) and the SYTO16 nucleic acid (final conc. 20 μM) fluorescence dye (Invitrogen) were used for staining the EPS and live cells, respectively.

Fabrication of Microfluidic Device

The PDMS (polydimethyl siloxane) microfluidic device was fabricated by soft lithography[19,20]. The microfluidic channel was 2 cm long, 1 cm wide and 400 μm deep and contained 1 inlet and 1 outlet. The SYLGARD® 184 silicone kit was purchased from Dow Corning and the PDMS layer fabricated to have the same design as the microfluidic device was prepared with a ratio of 1 : 10 (curing agent : PDMS) as describe elsewhere[19]. The surfaces of the PDMS layer and a microscope slide glass were simultaneously treated in an O_2 plasma (Harrick Scientific, Ithaca, NY, USA) at 50 Watts for 40 seconds and the two surfaces were then brought together to form an irreversible bond. Access ports (inlet and outlet) were prepared by punching and tygon tubes (ID=1 mm, Fisher Scientific International Inc., Hampton, NH, USA) were inserted through these ports to supply the bacterial culture and fresh media. A syringe pump (KD scientific, Holliston, MA, USA) was connected through the tubing to continuously supply media into the channel.

Growth Rate and pH Measurement

The pre-culture of *S. mutans* was prepared by inoculating the single colony from the BHI agar plate into 5 mL TSB broth and incubating at 37°C and 220 rpm overnight. Planktonic growth rates of the strain were measured by measuring the optical density at 600 nm. Changes in pH were monitored during both planktonic and biofilm stages, using a pH meter (pH 56, Martini Instruments Co. USA).

Biofilm Formation in the Microchannel

The biofilm of *S. mutans* was formed as described by Lim *et al*.[19] with some modification. In brief, the *S. mutans* pre-culture was incubated in fresh TSB medium and grown to an $O.D_{600}$ of 0.5. The microchannel was washed twice with fresh TSB medium and then filled with the pre-culture. The device was incubated for 30 min at room temperature to allow some cells in the microchannel to attach to the glass surface. After attachment, the air tight syringe pump was connected to the device through the inlet and started to continuously flow fresh TSB medium with or without $Fe_2(SO_4)_3$ at 5 μL min^{-1} at room temperature.

Staining EPS, Live Cells and Ferric Ions in the Biofilms with Fluorescent Dyes

To visualize the EPS and live cells in the biofilms, the biofilm formed in the chip was stained with 20 μg mL^{-1} Con A-Rho and 20 μM SYTO16 fluorescence dye, respectively. The staining procedure was modified from previously published methods[21,22]. In detail, unbound cells in the microchannel were first washed out by flowing PBS solution for 30 min at 5 μL min^{-1}. The Con A-Rho solution was then flown into the microchannel for 30 min at the same flow rate. Excess Con A-Rho dye was removed by flowing PBS into the channel again. Similarly, live cells in the biofilms were stained with SYTO16 dye and unbound dye was removed with PBS solution. Independent experiments were performed and different images were collected for analysis.

A ferric chemosensor[18] (final conc. 1 μM), which is quenched upon binding with a ferric ion, was used to stain ferric ions that had accumulated in the biofilm. The biofilm was stained using the same procedure described for the other fluorescent dyes. Since the chemosensor intensity is affected by changes in pH, the pH during the entire biofilm development stages was carefully and consistently monitored.

CLSM Imaging

Fluorescent images of the biofilms were obtained using confocal laser scanning microscopy (CLSM) (LSM 510, Zeiss)[23]. Digital image analysis of the CLSM optical thin sections was performed with the Zeiss LSM software. Fluorescent images were acquired at excitation wavelengths of 543 nm and 488 nm and emission wavelengths of 527 nm and 488 nm for Con A-Rho and SYTO16, respectively. To quantify the number of viable cells, fluorescence intensities from the confocal images were analyzed using image analysis software, image J (NIH, USA)[20]. The fluorescent intensity of ferric was analyzed using the same method describe earlier. The fluorescence intensity of light was measured in arbitrary unit.

Acknowledgements

This work was supported by the Korea Science and Engineering Foundation (KOSEF) grant funded by

the Korea government (MEST) (No. R01-2008-000-20593-0) and W. Shumi is supported by EGPP (Ewha Global Partnership Program). J. Lim and S.H. Kim were supported by BK21 program (2008) and the Seoul R&BD Program (2008).

References

1. Zaura, E. & Cate, J.M. Dental plaque as a biofilm: A pilot study of the effect of nutrients on plaque pH and dentin demineralization. *Caries Res.* **38**, 9-15 (2004).
2. Jakubovics, N.S., Stromberg, N., Dolleweerd, C.J., Kelly, C.G. & Jenkinson, H.F. Differential binding specificities of oral streptococcal antigen I/II family adhesins for human or bacterial ligands. *Mol. Microbiol.* **55**, 1591-1601 (2005).
3. Lemos, J.A.C., Abranches, J. & Burne, R.A. Responses of cariogenic *Streptococci* to environmental stresses. *Curr. Issues Mol. Biol*. **7**, 95-108.
4. Thomas, J.G. & Nakaishi, L.A. Managing the complexity of a dynamic biofilm. *JADA*. **137**, 10S-15S (2006).
5. Sutherland, I.W. Biofilm exopolysaccharides: a strong and sticky framework. *Microbiol*. **147**, 3-9 (2001).
6. Matsuyama, J., Sato, T., Hoshino, E., Noda, T. & Takahashi, N. Fermentation of five sucrose isomers by human dental plaque bacteria. *Caries Res*. **37**, 410-415 (2003).
7. Zhang, T. & Fang, H.H.P. Quantification of extracellular polymeric substances in biofilms by confocal laser scanning microscope. *Biotechnol. Lett.* **23**, 405-409 (2001).
8. Scheie, A.A. Mechanisms of dental plaque formation. *Adv. Dent. Res.* **8**, 246-253 (1994).
9. Yoshida, A. & Kuramitsu, H.K. Multiple *Streptococcus mutans* genes are involved in biofilm formation. *Appl. Environ. Microbiol.* **68**, 6283-6291 (2002).
10. Singleton, S. *et al*. Methods for microscopic characterization of oral biofilms: Analysis of colonization, microstructure, and molecular transport phenomena. *Adv. Dent. Res.* **11**, 133-149 (1997).
11. Leme, A.F.P., Koo, H., Bellato, C.M., Bedi, G. & Cury, J.A. The role of sucrose in cariogenic dental biofilm formation-new insight. *J. Dent. Res*. **85**, 878-887 (2006).
12. Francesca, B. *et al*. Both lactoferrin and iron influence aggregation and biofilm formation in *Streptococcus mutans*. *Biometals* **17**, 271-278 (2004).
13. Pecharki, G.D. *et al*. Effect of sucrose containing iron (II) on dental biofilm and enamel demineralization *in situ*. *Caries Res*. **39**, 123-129 (2005).
14. Espósito, B.P., Breuer, W. & Cabantchik, Z.I. Design and applications of methods for fluorescence detection of iron in biological systems. *Biochem. Soc. Trans.* **30**, 729-732 (2002).
15. Spatafora, G., Moore, M., Landgren, S., Stonehouse, E. & Michalek, S. Expression of *Streptococcus mutans* fimA in iron-responsive and regulated by a DtexR homologue. *Microbiol.* **147**, 1599-1610 (2001).
16. Thomas, F. *et al*. Calcein as a fluorescent probe for ferric iron: Applecation to iron nutrition in plant cells. *J. Biol. Chem.* **274**, 13375-13383 (1999).
17. Nudelman, R. *et al*. Molecular fluorescent-labeled siderophore analogues. *J. Med. Chem.* **41**, 1671-1678 (1998).
18. Jun, E.J., Kim, J., Swamy, K.M.K., Park, S. & Yoon J. A fluorescein derivative for nanomolar aqueous copper and monitoring copper ion uptake by transferrin and amyloid precursor protein. *Tetrahedron Lett.* **47**, 1051-1054 (2006).
19. Lim, J. *et al*. Nanoscale characterization of *Escherichia coli* biofilm formed under laminar flow using atomic force microscopy (AFM) and scanning electron microscopy (SEM). *Bull. Korean Chem. Soc.* **29**, 2114-2118 (2008).
20. Nam, S.W., van Noort, D. & Park, S. Use of a microvalve-controlled microfluidic device in a chemotaxis assay of *Tetrahymena pyriformis* in response to amino acids released from bacteria. *Biochip J.* **1**, 111-116 (2007).
21. Kreth, J. *et al*. Quantitative analysis of *Streptococcus mutans* biofilms with quartz crystal micrbalance, microjet impingement and confocal microscopy. *Biofilms* **1**, 227-284 (2004).
22. Tam, K. *et al*. Real-time monitoring of *Streptococcus mutans* biofilm formation using a quartz crystal microbalance. *Caries Res*. **41**, 474-483 (2007).
23. Chen, M., Lee, D., Tay, J. & Show, K. Staining of extracellular polymeric substances and cells in bioaggregates. *Appl. Microbiol. Biotechnol.* **75**, 467-474 (2007).